Magnetism of Rapidly Quenched $Sm_{1-x}Zr_xCo_5$ Nanocrystalline Materials

W. Y. Zhang[1,2], S. Valloppilly[2], X. Z. Li[2], Y. Liu[1,2], S. Michalski[1,2], T. A. George[1,2], R. Skomski[1,2], J. E. Shield[2,3], and D. J. Sellmyer[1,2]

[1]Department of Physics and Astronomy, University of Nebraska, Lincoln, NE 68588 USA
[2]Nebraska Center for Materials and Nanoscience, University of Nebraska, Lincoln, NE 68588 USA
[3]Department of Mechanical and Materials Engineering, University of Nebraska, Lincoln, NE 68588 USA

The effect of Zr addition on nanostructure and magnetic properties in nanocrystalline $Sm_{1-x}Zr_xCo_5$ ($x = 0 - 0.6$) has been investigated. (Sm, Zr)Co_5 with the $CaCu_5$ structure was synthesized by melt spinning. The lattice parameters a and b decrease with x, whereas c increases. Thus, the unit cell volume of (Sm, Zr)Co_5 shrinks because the smaller Zr atoms occupy the sites of the larger Sm atoms. Zr addition decreases the grain size and induces the formation of planar defects. The coercivity decreases with x, due to weakening of magnetocrystalline anisotropy energy and effective intergrain exchange coupling. A very high coercivity of 39 kOe and energy product of 13.9 MGOe are obtained for $x = 0$. The remanence of (Sm, Zr)Co_5 increases with x. For $x \leq 0.4$, the energy product slightly decreases with x. The results show that 40% of the Sm can be replaced by the less expensive Zr, with an energy-product reduction of only 10%. In addition, the planar defects are responsible for the change of coercivity mechanism from the nucleation-type of reverse domain for the $x = 0$ to the pinning-type of domain wall for the $x = 0.4$.

***Index Terms*—Coercivity, magnetic property, nanomaterials, rare-earth transition-metals compounds.**

I. Introduction

$SmCo_5$ with the $CaCu_5$ structure has attracted tremendous attention due to its high magnetocrystalline anisotropy and Curie temperature [1], [2]. Sm is a key rare-earth (R) element that is relatively expensive. Reducing the Sm content in $SmCo_5$ may help to reduce material cost and extend the range of applications. It was reported that rare-earth elements can be partially replaced by non-rare-earth elements such as Zr, Ti, and Hf to improve magnetic properties of permanent-magnet materials [3]–[7]. For example, the remanence of rapidly-quenched $R_2Fe_{14}B$ was enhanced by replacing R with 2 at% Zr. The Curie temperature of $PrCo_5$ increases 29 K after 10 at% Ti was added. Based on the Sm-Co binary phase diagram [8], a high cooling rate is required to prevent the decomposition of $SmCo_5$ to Sm_2Co_{17} and Sm_5Co_{19} at 812°C, which have low magnetocrystalline anisotropies and are detrimental to magnetic properties. In this work, Sm-lean single-phase $Sm_{1-x}Zr_xCo_5$ ($x = 0-0.6$) was fabricated by melt spinning. The relationships between the structure and magnetic properties were studied.

II. Experimental Method

Ingots of $Sm_{1-x}Zr_xCo_5$ ($x = 0-0.6$) were arc melted from high-purity elements in an argon atmosphere. The ribbons were made by ejecting molten ingots in a quartz tube onto the surface of a rotating copper wheel with a speed of 40 m/s. The typical size of ribbons is 2 mm wide and 50 μm thick. The phase components were determined by a Rigaku D/Max-B X-ray diffraction (XRD) system. The magnetic properties were measured by a superconducting quantum interference device (SQUID) magnetometer at fields up to 7 T. The applied field was parallel to the long direction of the ribbon.

Manuscript received October 22, 2012; accepted January 11, 2013. Date of current version July 15, 2013. Corresponding author: W. Y. Zhang (e-mail: wenyong.zhang@unl.edu).

Color versions of one or more of the figures in this paper are available online at http://ieeexplore.ieee.org.

Digital Object Identifier 10.1109/TMAG.2013.2240440

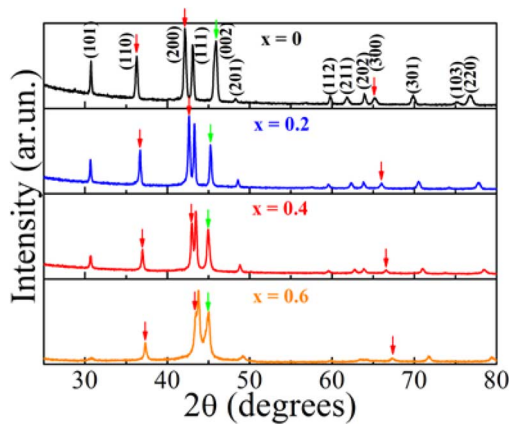

Fig. 1. XRD patterns of $Sm_{1-x}Zr_xCo_5$ ($x = 0 - 0.6$).

III. Results and Discussion

Fig. 1 shows XRD patterns of $Sm_{1-x}Zr_xCo_5$. The diffraction peaks of all the samples were indexed as single-phase (Sm, Zr)Co_5 with the $CaCu_5$ structure. The relative intensity of the (200) peak becomes weaker with the increase of x. However, the relative intensity of (111) peak becomes stronger. For $x = 0.6$, the intensity of the diffraction peak of (111) is strongest, which is the characteristic of isotropic $SmCo_5$ [9]. This indicates that Zr addition restrains the (200) preferred orientation and changes the ribbons from anisotropic to isotropic. The (200) and (300) peaks shift to higher angles with x as indicated by the red arrows on Fig. 1. At the same time, the (002) peak shifts to a lower angle with x (green arrow). These reflect the changes of the lattice parameters with x. The results are presented in Fig. 2. c increases with x but a decreases with x which causes the cell volume to shrink. This is because the smaller Zr atoms substitute the bigger Sm atoms in the lattice.

Fig. 3 shows the TEM images of $Sm_{1-x}Zr_xCo_5$ ($x = 0, 0.4$) and corresponding statistical distribution of grain size. Compared to the $x = 0$, the $x = 0.4$ has a smaller mean grain size

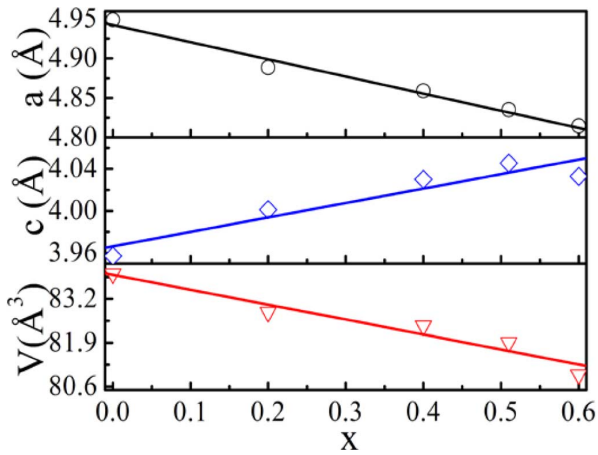

Fig. 2. Zr content dependence of the lattice parameters (a, c) and cell volume (V) for Sm_{1-x} Zr_x Co_5 $(x = 0 - 0.6)$.

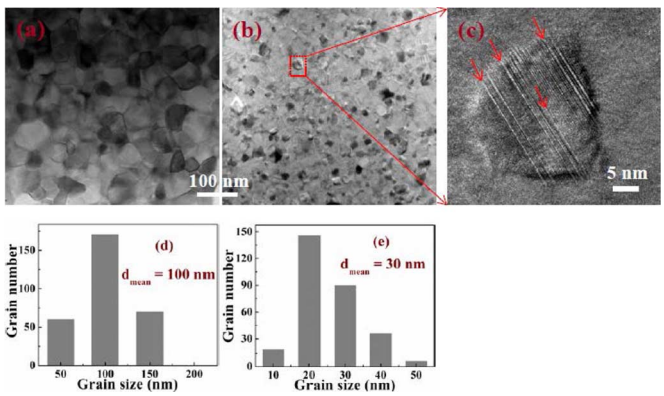

Fig. 3. TEM images of the Sm_{1-x} Zr_x Co_5 $(x = 0$ (a), 0.4 (b)), enlarged image of the $x = 0.4$ (c), and the statistical distribution of grain size of the $x = 0$ (d) and $x = 0.4$ (e).

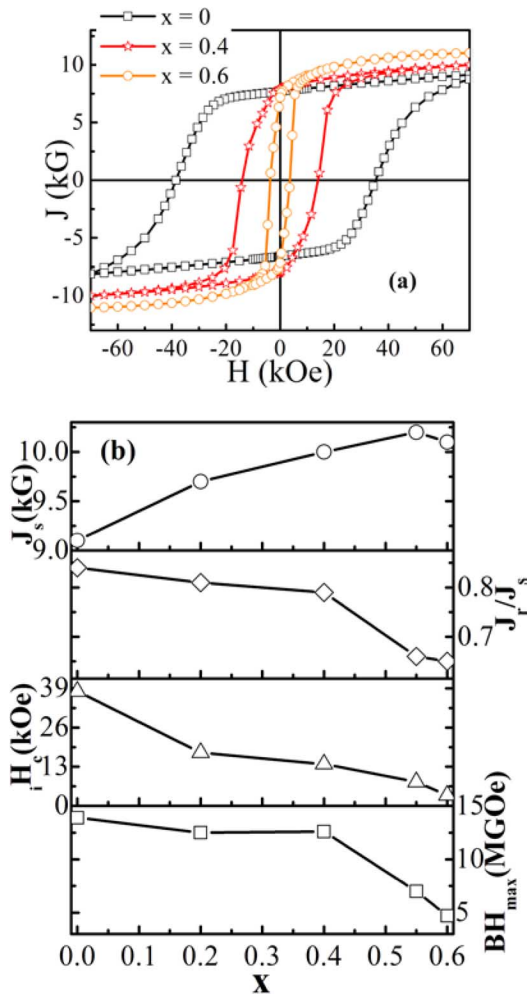

Fig. 4. Hysteresis loops of Sm_{1-x} Zr_x Co_5 $(x = 0 - 0.6)$ (a) and deduced magnetic properties (b): saturation magnetization (J_s), remanence ratio (J_r/J_s), coercivity $({}_iH_c)$, and energy product $((BH)_{max})$.

and shallower size distribution. It reveals that Zr addition decrease the grain size and refine the nanostructure. In addition, the planar defects indicated by the red arrows in Fig. 3(e), which may be the stacking fault or antiphase domain wall, were observed in the $x = 0.4$. This indicates that Zr addition induces the formation of planar defects.

Fig. 4(a) shows the hysteresis loops of the Sm_{1-x} Zr_x Co_5 $(x = 0 - 0.6)$ ribbons. It is evident that magnetic properties of the samples are strongly dependent on Zr content. The magnetocrystalline anisotropy constant K, and the saturation magnetic polarization J_s of Sm_{1-x} Zr_x Co_5 $(x \geq 0.4)$ can be estimated using the law of the approach to saturation [10]. The magnetocrystalline anisotropy field was calculated as $H_a = 2$ K/M_s [10]. The value of the H_a for $x = 0.4$ and 0.6 are 39 and 31 kOe, respectively. The reported value of the H_a for $x = 0$ is 400 kOe [1]. Zr addition significantly reduces H_a. It is reported that 60% of the anisotropy energy K of $SmCo_5$ is due to samarium [11], so the decrease of Sm concentration leads to the reduction of anisotropy field. The deduced magnetic properties are shown in Fig. 4(b). The substitution of Zr for Sm may decrease the number of electron transferring from 5d/6s band of Sm to 3d band of Co. And thus the saturation polarization increases with x. Zr addition reduces the preferred orientation of c-axis of hard phase, as shown in Fig. 1, thus the remanence ratio decreases with x. The decrease of coercivity with x is attributed to the reduction of the magnetocrystalline anisotropy of the hard magnetic phase. The energy product decreases only to 12.5 MGOe with a 40% Zr substitution. The very high coercivity of 39 kOe and maximum energy product of 13.9 MGOe were achieved for $x = 0$.

Generally, the coercivity mechanism of permanent-magnet materials can be determined by comparing initial magnetization curves and applied field dependence of coercivity [12]–[15]. Fig. 5 shows the initial magnetization curves for Sm_{1-x} Zr_x Co_5 $(x = 0, 0.4)$ and applied field dependence of the coercivity. For $x = 0$, the magnetization and coercivity increase rapidly at low field. They approach saturation at the low field of 7 and 15 kOe, respectively, which are much smaller than the saturated coercivity. This indicates that domain walls move easily, and the coercivity is controlled by the nucleation of reverse domains. A similar phenomenon was observed in annealed 5 m/s $Sm_{1.1}$ Co_5 ribbons [13]. For $x = 0.4$, the magnetization and coercivity increase slowly until the applied field exceeds a critical value comparable to the saturated coercivity where they increase faster. The saturation of the magnetization and coercivity

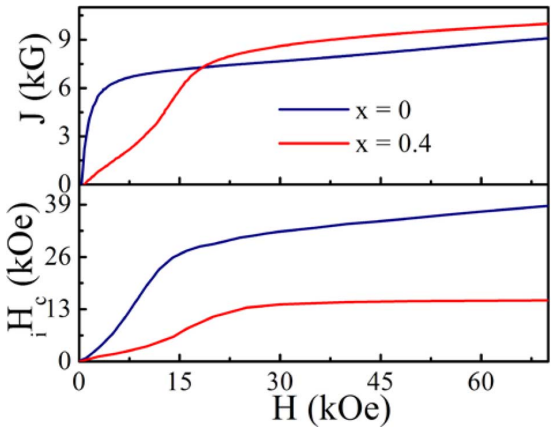

Fig. 5. Initial magnetization curves for Sm_{1-x} Zr_x Co_5 $(x = 0, 0.4)$ and applied field dependence of coercivity.

is completed at the fields much higher than the saturated coercivity. A shoulder appears in the initial magnetization and ${}_iH_c$-H curves. This implies that domain walls cannot move freely, and coercivity is governed by the pinning of domain walls. The planar defects shown in Fig. 3(e) behave as pinning centers and are responsible for the change of the coercivity mechanism.

IV. Conclusion

Sm-lean Sm_{1-x} Zr_x Co_5 $(x = 0 - 0.6)$ alloys were fabricated by the melt-spinning technique, and lattice parameters of (Sm, Zr)Co_5 are dependent on Zr content. The unit cell volume shrinks with the increase of Zr content. Zr addition was found to refine the nanostructure and induce the formation of planar defects. The saturation magnetization of (Sm, Zr)Co_5 increases with the addition of limited amount of Zr, which may result from the reduction of the number of electron transferring from 5d/6s band of Sm to 3d band of Co. The remanence ratio and coercivity decrease with x. The energy product slightly decreases with the increase in Zr content $(x \leq 0.4)$. Therefore, a proper Zr addition leads to improvement of the performance vs price ratio of (Sm, Zr)Co_5, which could be useful to extend the range of the applications. In addition, Zr addition changes the coercivity mechanism of the sample from the nucleation of reverse domains to the pinning of domain walls due to the existence of planar defects.

Acknowledgment

This research was supported by DOE-BES (DJS, RS, YL), ARPA-E (WYZ, JS), ARO (TAG) and NCMN (SV).

References

[1] K. Kumar, "$RETM_5$ and RE_2 TM_{17} permanent magnets development," *J. Appl. Phys.*, vol. 63, pp. R13–R57, Nov. 1988.

[2] H. Ido, K. Konno, H. Ogata, K. Sugiyama, H. Hachino, M. Date, and K. Maki, "Magnetic study of $SmCo_5$, $PrCo_5$, $SmCo_4$ B, and Sm_3 Co_{11} B_4 under pulse high field," *J. Appl. Phys.*, vol. 70, pp. 6128–6130, Nov. 1991.

[3] Z. Chen, B. R. Smith, D. N. Brown, and B. M. Ma, "Effect of Zr substitution for rare earth on microstructure and magnetic properties of melt-spun $(Nd_{0.75}$ $Pr_{0.25})_{12.5-x}$ Zr_x Fe_{82} $B_{5.5}$ $(x = 0 - 3)$ ribbons," *J. Appl. Phys.*, vol. 91, pp. 8168–8170, May 2002.

[4] M. Zinkevich, N. Mattern, I. Bächer, and S. Puerta, "Formation, crystal structure and magnetic properties of (1:12) compounds in the Fe-Gd-Mo-Zr system," *J. Alloys Comp.*, vol. 336, pp. 320–328, Apr. 2002.

[5] H. O. Gupta and W. E. Wallace, "Magnetic behavior of Pr_{1-x} M_x Co_5 compounds (M = Ti, Zr and Hf)," *J. Magn. Magn. Mater.*, vol. 50, pp. 339–342, July 1985.

[6] W. Y. Zhang, C. H. Chiu, L. C. Zhang, K. Biswas, H. Ehrenberg, W. C. Chang, and J. Eckert, "Complete suppression of metastable phase and significant enhancement of magnetic properties of B-rich PrFeB nanocomposites prepared by devitrifying amorphous ribbons," *J Magn. Magn. Mater.*, vol. 308, pp. 24–27, Jan. 2007.

[7] T. W. Capehart, R. K. Mishra, and F. E. Pinkerton, "Determination of the zirconium site in zirconium-substituted Nd_2 Fe_{14} B," *J. Appl. Phys.*, vol. 73, pp. 6476–6478, May 1993.

[8] H. Okamoto, "Co-Sm (cobalt-samarium)," *J. Phase Equilibria*, vol. 20, pp. 535–536, Sept. 1999.

[9] A. R. Yan, W. Y. Zhang, H. W. Zhang, and B. G. Shen, *J. Magn. Magn. Mater.*, vol. 210, pp. L10–L14, Feb. 2000.

[10] G. C. Hadjipanayis, D. J. Sellmyer, and B. Brant, "Rare-earth-rich metallic glasses. I. Magnetic hysteresis," *Phys. Rev. B*, vol. 23, pp. 3349–3354, Apr. 1981.

[11] R. Skomski and J. M. D. Coey, *Permanent Magnetism*. Bristol, U.K.: IOP Publishing, Dec. 1999, p. 275.

[12] D. J. Sellmyer, Y. F. Xu, M. L. Yan, Y. C. Sui, J. Zhou, and R. Skomski, "Assembly of high-anisotropy $L1_0$ FePt nanocomposite films," *J. Magn. Magn. Mater.*, vol. 303, pp. 302–308, Aug. 2006.

[13] J. D. Livingston, "A review of coercivity mechanisms," *J. Appl. Phys.*, vol. 52, pp. 2544–2548, Mar. 1981.

[14] A. R. Yan, W. Y. Zhang, H. W. Zhang, and B. G. Shen, "Magnetic properties of Sm- and Cu-doped oriented $SmCo_5$ ribbons prepared by melt spinning," *J. Appl. Phys.*, vol. 88, pp. 2787–2790, Sept. 2000.

[15] K. H. J. Buschow, "New developments in hard magnetic materials," *Rep. Prog. Phys.*, vol. 54, pp. 1123–1213, Sept. 1991.